Acupuncture and Herbal Medicine

Characterization of metabolic profiles of Lanqin Oral Liquid in rats by ultra-high-performance liquid chromatography tandem time-of-flight mass spectrometry

Yue-Yue Tan[1], Meng-Yuan Wang[1], Yu-Nuo Fan[1], Ya-Liu Fan[1], Ye Zhang[1], Bin Li[1], Yong-Xiang Wang[2], Hua Yang[1,*], Ping Li[1,*]

[1]*State Key Laboratory of Natural Medicines, School of Traditional Chinese Pharmacy, China Pharmaceutical University, Nanjing, China;*
[2]*Nanjing Hailing Traditional Chinese Medicine Pharmaceutical Technology Research Co., Ltd., Nanjing, Jiangsu, China*

Abstract

Objective: Lanqin oral liquid (LOL), as a traditional Chinese medicine prescription, has obvious clinical efficacy in the treatment of pharyngeal inflammation. Exploring the distribution of LOL prototype components and metabolites in plasma is of great significance for understanding potentially effective compounds. The aim of this study is to elucidate the metabolites and main metabolic pathways of LQL *in vivo*.

Methods: In this study, a reliable approach integrated background subtraction and mass defect filtering (MDF), based on quadrupole time-of-flight mass spectrometry (QTOF-MS) technology, was performed to systematically scan the metabolites of LOL in rat plasma. In addition, according to the prototype mass spectrometry fragmentation pattern and combined with metabolic pathway analysis, a biotransformation oriented analysis strategy was established and applied to the identification of metabolites in LOL *in vivo*.

Results: As a result, 159 compounds (58 prototypes and 101 metabolites) were identified or tentatively characterized in drug-containing plasma, including 74 flavonoids, 30 alkaloids, 34 terpenoids, five phenylpropanoids, six phenolic acids, five fatty acids, and five other type components. The main metabolic pathways include methylation, demethylation, hydroxylation, hydrogenation, glucuronidation, and sulfation.

Conclusions: This study provides an overall characterization of the metabolites of LOL *in vivo* for the first time, providing a solid material basis for exploring the therapeutic effects and pharmacological mechanisms of LOL.

Keywords: Background subtracts, Lanqin Oral Liquid, Mass defect filtering, Metabolic profiles, UHPLC-QTOF-MS

Graphical abstract: http://links.lww.com/AHM/A168.

Introduction

In recent years, research on the chemical components of traditional Chinese medicines (TCMs) has mainly relied on traditional methods of phytochemical separation and pharmacological screening[1]. Studies on serum pharmacology of TCMs have shown that constituents absorbed into the bloodstream and metabolites transferred from prototype components may have pharmacological effects[2–3]. Therefore, studying drug ingredients *in vivo* and revealing the bioactive components in TCM formulas have important biological significance.

Lanqin Oral Liquid (LOL) is a TCM prescription made up of five herbs, namely, *Gardeniae* Fructus, *Isatidis* Radix, *Sterculiae Lychnophorae* Semen, *Scutellariae* Radix and *Phellodendri Chinensis* Cortex. Pharmacological evidence shows that LOL has the effects of clearing heat and detoxifying, alleviating pharyngeal swelling, and facilitating swallowing, which is conducive to clinical application in the treatment of pediatrics, otolaryngological diseases, and upper respiratory tract infections[4]. For the *in vitro* component analysis of LOL, Wang et al.[5] streamlined a versatile 3D separation method to efficiently characterize the multicomponents in LOL by integrating ultra-high performance liquid chromatography-ion mobility-quadrupole time-of-flight mass spectrometry (UHPLC-IM-QTOF-MS) and in-house library of UNIFI, which tentatively identified 175 components. Fan et al.[6] established a database-oriented integration strategy, which resulted in the putative identification of 170 compounds. However,

Yue-Yue Tan and Meng-Yuan Wang contributed equally to this work.

**Corresponding author. Hua Yang, E-mail: yanghuacpu@126.com; Ping Li, E-mail: liping2004@126.com.*

Received 28 December 2023 / Accepted 11 February 2025

How to cite this article: *Tan Y-Y, Wang M-Y, Fan Y-N, Fan Y-L, Zhang Y, Li B, Wang Y-X, Yang H, Li P. Characterization of metabolic profiles of Lanqin Oral Liquid in rats by ultra-high-performance liquid chromatography tandem time-of-flight mass spectrometry. Acupunct Herb Med 2025;5(1):76–88. DOI: 10.1097/HM9.0000000000000149*

there have been no reports about the chemical analysis of LOL *in vivo* so far. Undoubtedly, for the sake of guiding its safe and effective clinical application, it is necessary to discover the *in vivo* chemical properties, especially the metabolic components, of LOL. In the study of metabolite identification using high-resolution mass spectrometry, the non-targeted analysis of metabolites in biological samples based on traditional data-dependent acquisition mode is often faced with serious background matrix interference. Metabolite ion information is annihilated in background noise and many endogenous interference ions in the biological matrix, so it is difficult to find and identify[7]. In addition to improving the detection sensitivity of mass spectrometry, the development of data analysis methods is also an effective means to expose the ion information of metabolites in complex systems.

As reported, many mass spectrometry data processing techniques have been applied and developed in the characterization and identification of TCM components. Commonly used data processing techniques reported in the literature include background subtraction[8], mass defect filtration[9], product ion/neutral loss filtration technology[10–11], isotope pattern filtration[12], mass spectral trees similarity filtration technology[13], database matching[14], etc. The application of these technologies in combination with computer and molecular network technology can largely eliminate the interference of endogenous substances in complex biological samples, which greatly improves the efficiency and accuracy of the identification of chemical components in TCMs. Among them, background subtraction technology combined with mass defect filtration, neutral loss, and other technologies are conducive to the capture of low-concentration metabolites[15], to conduct comprehensive and systematic characterization of Chinese medicine metabolites.

This study establishes a background deduction combined with a mass defect filtering (MDF) data analysis method for complex biological systems based on QTOF-MS technology. An analytical strategy guided by biotransformation was developed and used for the screening and characterization of metabolites in complex biological systems, which enriched the research on the metabolism of active ingredients in LOL. Finally, 159 components were preliminarily identified in this study, mainly including iridoids, alkaloids, and flavonoids, and the *in vivo* metabolic pathways of the chemical components in LOL were proposed. This investigation could provide a chemical basis for a pharmacological study on LOL.

Materials and methods

Chemicals and reagents

The reference substances of shanzhiside, geniposidic acid, genipin-1-gentiobioside, oroxylin A-7-*O*-glucuronide, 5-*O*-feruloylquinic acid, geniposide, phellodendrine, magnoflorine, *p*-coumaric acid, isoquercitrin, wogonoside, coptisine chloride, jatrorrhizine chloride, baicalin, berberrubine, palmatine chloride, berberine hydrochloride, norwogonin 7-*O*-glucuronide, calycosin, baicalein, wogonin, oroxylin A, genkwanin were purchased from Chengdu Push Biological Technology Co. Ltd. (Chengdu, China); (R,S)-goitrin, gardenoside, feretoside, 4-*O*-feruloylquinic acid, chrysin 6-*C*-arabinoside 8-*C*-glucoside, crocetin were obtained from Shanghai Yuanye Biological Technology Co. Ltd. (Shanghai, China); epiberberine, chrysin 7-*O*-glucuronide were obtained from Chengdu Must Biological Technology Co. Ltd. (Chengdu, China). The purity of the above reference substances is not less than 98%, and their details are shown in Supplementary Table S1 (http://links.lww.com/AHM/A164).

The prescription LOL (batch no. 22011581) was supplied by Yangtze River Pharmaceutical Group (Jiangsu, China). Formic acid was provided by ROE Scientific Inc. (Newark, DE, USA). Methanol and ACN (LC-MS grade) were purchased from Merck KGaA (Darmstadt, Germany). Deionized water (18.2 MΩ·cm) was prepared through the Milli-Q water purification system (Millipore, Milford, MA, USA).

Preparation of standard solutions

All standards were accurately weighed and configured to a final concentration of 1 mg/mL using methanol as the solvent. Mix different standard solutions in a certain proportion to obtain a mixed standard solution with appropriate concentration. All samples were laid at –80°C until the experiment.

Preparation of LOL

The freeze-dried powder obtained after freeze-drying of LOL (90 mL) solution was added to pure water (30 mL) for redissolution, vortex mixing, and centrifugation at 4,000 rpm for 10 minutes. Take the supernatant and store it in the refrigerator at 4°C for 24 h.

Animal experiment

Male Sprague-Dawley rats (6 weeks of age, 200–220 g) were obtained from Zhejiang Vital River Laboratory Animal Technology Co., Ltd. [license number: SCXK (Zhe) 2019-0001]. The animals are free access to standard water and food for a week to acclimate. The animals were placed in a barrier system with a 12-hour light cycle, constant humidity (50 ± 10)%, and temperature (22 ± 2)°C. The animal experiment protocol meets ethical requirements. The animal experiments were approved by the Department of Science and Technology Jiangsu Province (License No.: 2022-09-007) and conducted according to the guidelines of Provision and General Recommendation of Chinese Experimental Animals Administration Legislation.

After adapting to the environment for 7 days, the experiment can be conducted, and all rats could fast but drink water freely 12 h before the experiment. Randomly divide six rats into control group and LOL administration group, with 3 rats in each group. Administer a single dose of 7.2 mL/kg of concentrated LOL solution into rats by gavage. The dosage of LOL is equivalent to an eight-fold clinical dosage of 21.6 mL/kg (clinical dosage (2.7 mL/kg)). The control group was treated with water in parallel. Blood samples of approximately 200 μL were collected from the orbital venous plexus before (0 hours) and 0.5, 1, 2, 4, 6, 8, 12 and 24 h after administration. Immediately centrifuge the extracted blood sample at 4,000 rpm for 10 min at 4°C to prepare the plasma sample. All samples were stored in a –80°C freezer before analysis.

Preparation of plasma samples

At the same time point 100 µL plasma was incorporated for the characterization of maternal compounds and metabolites. The resulting 300 µL sample was mixed with acetonitrile (900 µL) at a ratio of 1:3 (V/V). Vortex the mixture for 5 min and centrifuge it at 13,000 rpm and 4°C for 10 min to precipitate proteins. Collect the supernatant and dry it under nitrogen gas. The dried sample was redissolved in 300 µL 70% methanol, swirled for 3 min, and then centrifuged at 13,000 rpm and 4°C for 10 min. Five microliter aliquots of the supernatant was injected into the UHPLC-QTOF-MS system for analysis.

Chromatographic separation and MS detection

Chromatographic separation was carried out on an Agilent series 1290 UPLC instrument (Agilent Technologies, Santa Clara, CA, USA), equipped with a column compartment, an autosampler, a diode-array detector, and a binary pump. Samples were separated on a Zorbax Eclipse Plus C18 column (RRHD) (2.1 mm × 100 mm, 1.8 µm). The mobile phase consisted of water with 0.1% (*v/v*) formic acid (phase A) and acetonitrile (phase B). The mobile phase gradient program is as follows: 0 min, 95% A; 1 min, 95% A; 3 min, 90% A; 15 min, 70% A; 23 min, 47% A; 30 min, 30% A; 37 min, 5% A; 42 minutes, 5% A. Set a post-processing time of 10 minutes to balance the column. Other parameters: injection volume: 5 µL; column temperature: 30°C; flow rate: 0.4 mL/min.

The Agilent 6530 QTOF MS (Agilent Technologies) equipped with a Dual Auto Jet Stream electrospray ionization source (ESI) was used for MS detection. Both negative and positive ion polarity modes were used for compound ionization. High-purity nitrogen was used as both drying gas and Sheath gas. The instrument parameters are set as follows: drying gas: N_2; drying gas flow: 10 L/min; drying gas temperature: 320°C; nebulizer: 35 psi; sheath gas: N_2; sheath gas flow: 11 L/min; sheath gas temperature: 350°C; mass range: MS: 100 to 1,500 *m/z*; MS/MS: 50 to 1,500 *m/z*; collision energy: 10, 20, 30, 40, 50,60 eV; OCT 1 RF: 750 V; fragmentor: 135 V; skimmer: 65 V; VCap: 4,000 V. To ensure the accuracy of TOF quality, a low-concentration tuning mixture of ESI (Agilent Technologies) is used for quality calibration/inspection before daily analysis.

Data processing and analysis

Data acquisition and analysis were operated on MassHunter Acquisition Software Version B.06.01 (Agilent Technologies) and Qualitative Analysis Software Version B.07.00, respectively (Agilent Technologies).

Use Agilent Mass Profiler Professional Version B.12.5 (Agilent Technologies) to post-process the collected raw data to eliminate background interference and generate mass lists. The processing parameters were set as bellows: minimum absolute abundance 500 counts; minimum number of ions 2; multiple charge states forbidden; retention time correction: maximum allowed RT shift 0.5% ± 0.5 minutes, mass window: 20 ppm ± 2.00 mDa; compound alignment: RT window 0.0% ± 0.3 minutes, mass window: 20 ppm ± 2.00 mDa; normalization algorithm: percentile shift; percentile shift: 75.0; find unique entities for analysis; baseline to median of all samples.

Results and discussion

For the sake of accurately and comprehensively obtaining the mass spectrometry information of prototypes and metabolites in complex biological systems, a screening strategy for the prototypes and their metabolites including background subtraction and metabolic MDF was developed. It is applied to the identification of LOL metabolites in rats.

Establishment of MDF windows

By observing the composition distribution of LOL *in vitro* and the metabolism of the main components of *Scutellaria baicalensis*[16–18], *Cortex Phellodendri*[19–21], and *Gardenia jasminoides*[22–23] *in vivo*, the MDF windows were constructed based on baicalin, berberine, and genipin, respectively, for flavonoid glycosides and aglycone compounds, isoquinoline alkaloids, iridoid glycosides, and aglycone compounds.

MDF window of alkaloids

The alkaloids in LOL are mainly derived from *Phellodendron amurense*, and quaternary ammonium alkaloids are the main ones. Berberine is a very well-known isoquinoline alkaloid, and its metabolism *in vivo* is relatively more studied[24–25]. Therefore, a screening window suitable for isoquinoline alkaloids was

Table 1

Common reactions of isoquinoline alkaloids *in vivo*

	Common metabolic reaction	Elemental composition change	Mass change (Da)	Reaction times parameter
a	Demethylation	$-CH_2$	–14.0157	0, 1, 2
	Demethylene	-C	–12.0000	0, 1
	Dehydrogenation	$-H_2$	–2.0157	0, 1
	Hydroxylation	+O	15.9949	0, 1, 2, 3
	Methylation	$+CH_2$	14.0157	0, 1, 2
	Reduction	$+H_2$	2.0157	0, 1, 2
b	Sulfation	$+SO_3$	79.9568	1
c	Glucuronidation	$+C_6H_8O_6$	176.0321	1
d	Sulfation + glucuronidation	$+C_6H_8O_9S$	255.9889	1

Table 2

Original datapoints and shifted datapoints at the boundary of isoquinoline alkaloids in MDF windows

		Original datapoints in windows		Shifted datapoints (coordinate change)	
Order*	Boundary of distribution area	*x*-axis†	*y*-axis‡	*x*-axis	*y*-axis
a					
1	Top	356	0.1864	355(–1)	0.1914(+0.005)
2	Top	368	0.1864	367(–1)	0.1914(+0.005)
3	Top	416	0.1711	417(+1)	0.1761(+0.005)
4	Top	410	0.1240	411(+1)	0.1290(+0.005)
5	Bottom	354	0.0612	355(+1)	0.0562(–0.005)
6	Bottom	342	0.0612	343(+1)	0.0562(–0.005)
7	Bottom	294	0.0765	293(–1)	0.0715(–0.005)
8	Bottom	300	0.1236	299(–1)	0.1186(–0.005)
b (sulfation)					
9	Top	436	0.1432	435(–1)	0.1482(+0.005)
10	Top	448	0.1432	447(–1)	0.1482(+0.005)
11	Top	496	0.1279	497(+1)	0.1329(+0.005)
12	Top	490	0.0808	491(+1)	0.0858(+0.005)
13	Bottom	434	0.0180	435(+1)	0.0130(–0.005)
14	Bottom	422	0.0180	423(+1)	0.0130(–0.005)
15	Bottom	374	0.0333	373(–1)	0.0283(–0.005)
16	Bottom	380	0.0804	379(–1)	0.0754(–0.005)
c (glucuronation)					
17	Top	532	0.2185	531(–1)	0.2235(+0.005)
18	Top	544	0.2185	543(–1)	0.2235(+0.005)
19	Top	592	0.2032	593(+1)	0.2082(+0.005)
20	Top	586	0.1561	587(+1)	0.1611(+0.005)
21	Bottom	530	0.0933	531(+1)	0.0883(–0.005)
22	Bottom	518	0.0933	519(+1)	0.0883(–0.005)
23	Bottom	470	0.1086	469(–1)	0.1036(–0.005)
24	Bottom	476	0.1557	475(–1)	0.1507(–0.005)
d (sulfation and gucuronidation)					
25	Top	612	0.1753	611(–1)	0.1803(+0.005)
26	Top	624	0.1753	623(–1)	0.1803(+0.005)
27	Top	672	0.1600	673(+1)	0.1650(+0.005)
28	Top	666	0.1129	667(+1)	0.1179(+0.005)
29	Bottom	610	0.0501	611(+1)	0.0451(–0.005)
30	Bottom	598	0.0501	599(+1)	0.0451(–0.005)
31	Bottom	550	0.0654	549(–1)	0.0604(–0.005)
32	Bottom	556	0.1125	555(–1)	0.1075(–0.005)

MDF: Mass defect filtering.

*Order: Connection order of shifted boundary data points: from 1 to 8; from 9 to 16; from 17 to 24; from 24 to 32.

†*x*-axis: Integral masses of data points.

‡*y*-axis: Decimal masses of data points.

constructed based on the metabolic reaction of berberine *in vivo*, and it was applied to screen metabolites of isoquinoline alkaloids in LOL.

Berberine ($C_{20}H_{18}NO_4^+$, calculated *m/z* 336.1236) usually undergoes the same or different metabolic reactions several times in the body, as shown in Table 1. Based on the structure of alkaloids, these reactions are arranged and combined to obtain a series of theoretical mass values. It should be noted that the mass change caused by sulfation and/or glucuronidation is larger than other simple reactions. To screen more reliably, four screening windows **a**, **b**, **c**, and **d** were constructed, respectively.

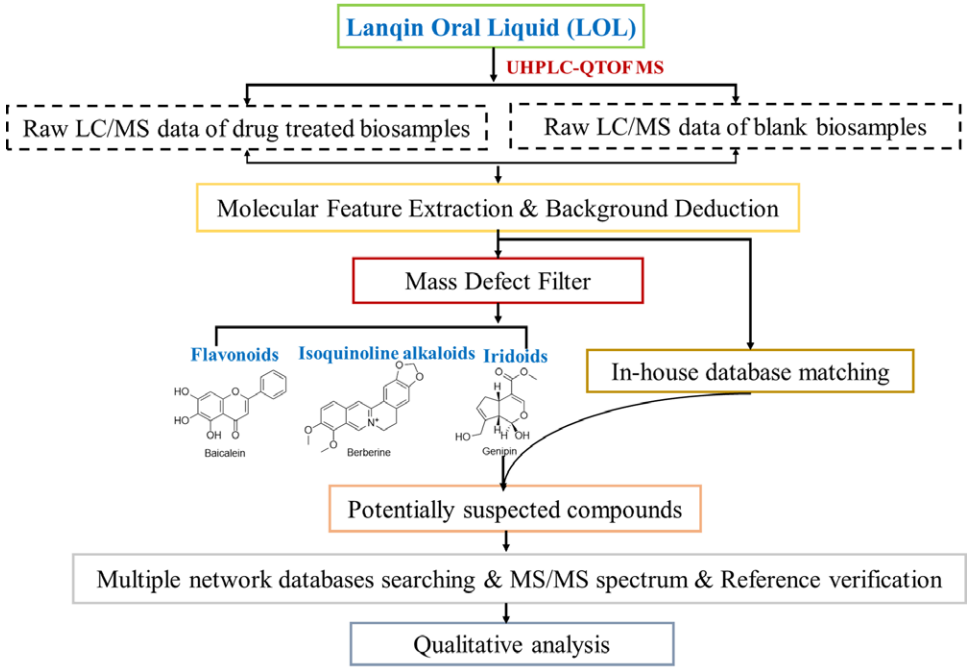

Figure 1. Overall strategy for metabolite identification of LOL. MS: Mass spectrometry; UHPLC-QTOF MS: Ultra-high performance liquid chromatography-quadrupole time-of-flight mass spectrometry.

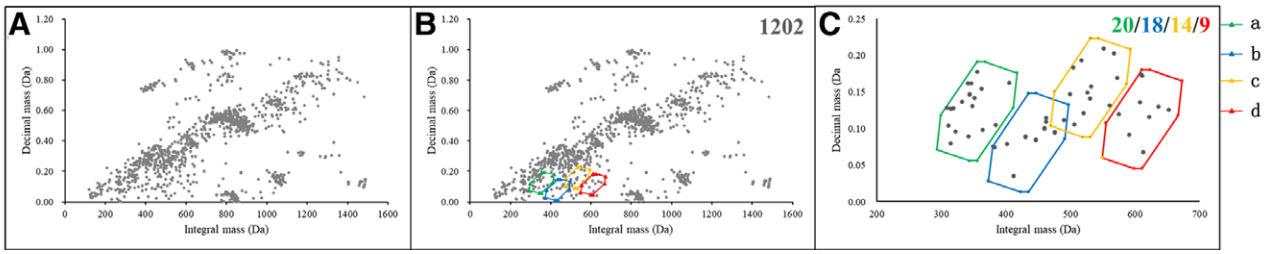

Figure 2. The process of screening potential isoquinoline alkaloids by MDF in positive mode. (A) The positive ions extracted of drug-containing plasma. (B) Candidate ions of alkaloids. (C) Target ions of alkaloids. MDF: Mass defect filtering.

Window **a** indicates that one or more simple reactions occur, and windows **b**, **c**, and **d** indicate that sulfation, glucuronidation, sulfation, and glucuronidation reactions occur, respectively, based on the formed window **a**.

Decompose all theoretical masses into integral masses and decimal masses in a two-dimensional coordinate system. Screen out eight edge values and construct a heptagonal MDF filtering window by sequentially connecting offset points. Due to measurement errors in mass spectrometry, the boundary points are slightly offset (horizontal± 1 Da, vertical ± 0.005 Da) to ensure fault tolerance. The detailed information is shown in Table 2. Therefore, the constructed MDF window of isoquinoline alkaloids was applied to screening as shown in Figure 2.

MDF window of flavonoid aglycones and glycosides

Combining the structure of flavonoid components and the phase I and phase II biotransformation pathways in biological systems to construct multiple MDF windows, the flavonoids in LOL have a parent nucleus scaffold of 2-phenylchromone, and the parent nucleus usually has a maximum of seven substituents, mainly with substituents of hydroxyl or methoxy[26].

Based on the identification results of the chemical composition *in vitro* of LOL and the analysis of the chemical composition *in vivo*, phase I metabolic reactions such as demethylation, hydroxylation, dehydroxylation, and hydrogenation reduction in organisms and phase II metabolic reactions such as methylation, glucuronidation, and sulfation were mainly undergone[16–18,27]. Therefore, according to baicalein ($C_{15}H_{10}O_5$, calculated *m/z* 270.0528) and its possible metabolic reactions (as shown in Supplementary Table S2, http://links.lww.com/AHM/A164), MDF windows for prototypes and metabolites of flavonoids aglycone were established (as shown in Figure 3A–C, G–I). The detailed information on boundary points is displayed in Supplementary Table S3 (http://links.lww.com/AHM/A164).

In addition, flavonoid glycosides are mainly connected by the hydroxyl group of flavonoid aglycones with glucuronic acid (+$C_6H_8O_6$, +176.0321 Da), glucose groups (+$C_6H_{10}O_5$, +162.0528 Da), and rhamnose groups (+$C_6H_{10}O_4$, +146.0579 Da). Based on the theoretical mass of flavonoid aglycone prototypes and metabolites, the theoretical mass values of flavonoid aglycone connecting these three glycosyl groups were calculated. The MDF windows of flavonoid glycosides were constructed

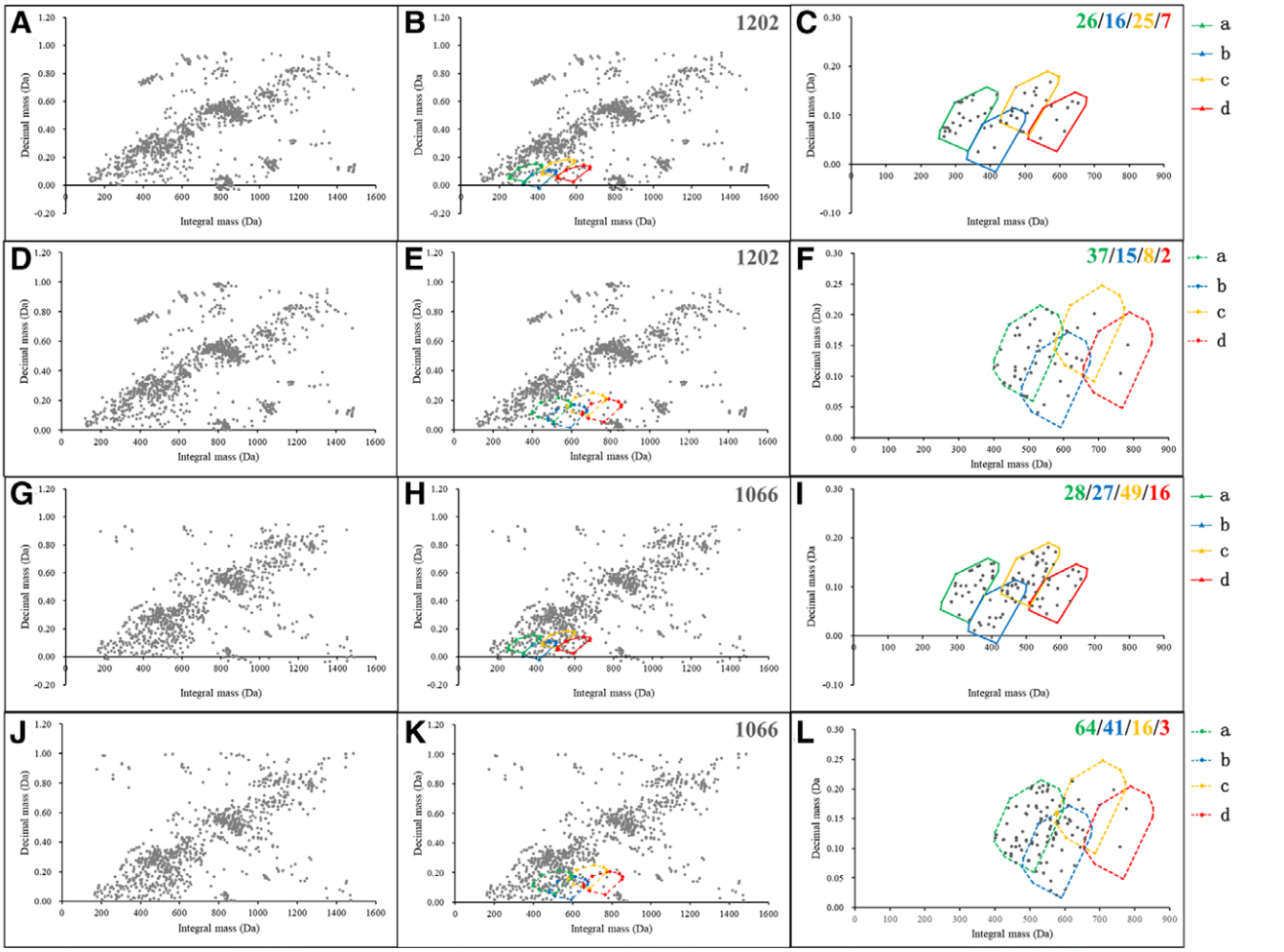

Figure 3. The process of screening potential flavonoids by MDF. (A–C) The process of screening potential flavonoid aglycones in positive mode. (D–F) The process of screening potential flavonoid glycosides in positive mode. (G–I) The process of screening potential flavonoid aglycones in negative mode. (J–L) The process of screening potential flavonoid glycosides in negative mode. MDF: Mass defect filtering.

as shown in Figure 3D–F, J–L. The detailed information on boundary points is displayed in Supplementary Table S4 (http://links.lww.com/AHM/A164).

MDF window of iridoid aglycones and glycosides

For iridoid aglycones, a multistage MDF window of iridoid aglycones was constructed according to genipin ($C_{11}H_{14}O_5$, calculated *m/z* 226.0841) and its metabolic reactions (as shown in Supplementary Table S2, http://links.lww.com/AHM/A164). The detailed information on boundary points is displayed in Supplementary Table S5 (http://links.lww.com/AHM/A164). The construction of the screening window for iridoid glycosides was similar to that of MDF windows for flavonoid glycosides (as shown in Figure 4). The detailed information on boundary points is displayed in Supplementary Table S6 (http://links.lww.com/AHM/A164).

Screening potential metabolites of LOL

The main purpose of this strategy is to eliminate interfering substances and quickly discover potential target compounds in complex biological samples. The suspected compounds were identified and confirmed through characteristic fragment matching and multiple database searches. As shown in Figure 1, first, all components detected in the plasma sample were obtained through mass spectrometry peak alignment and extraction. Second, endogenous components are deducted and MDF is performed to screen for potential target compounds. Finally, the screened compounds were characterized by matching the characteristic ion fragments and searching network database.

Step1: background subtraction

Preliminary data post-processing was performed on the collected raw data with mass profiler professional for peak detection and peak alignment. The interference of biological matrix was eliminated by finding the differential ions between blank plasma and drug-containing plasma. The results of the Wayne diagram show that in positive mode 1,202 differential compounds were discovered and 1,066 differential compounds were discovered in negative mode. These compounds unique to the dosing group were considered potential candidate compounds, and these compounds were subsequently processed by metabolic MDF and matching with database.

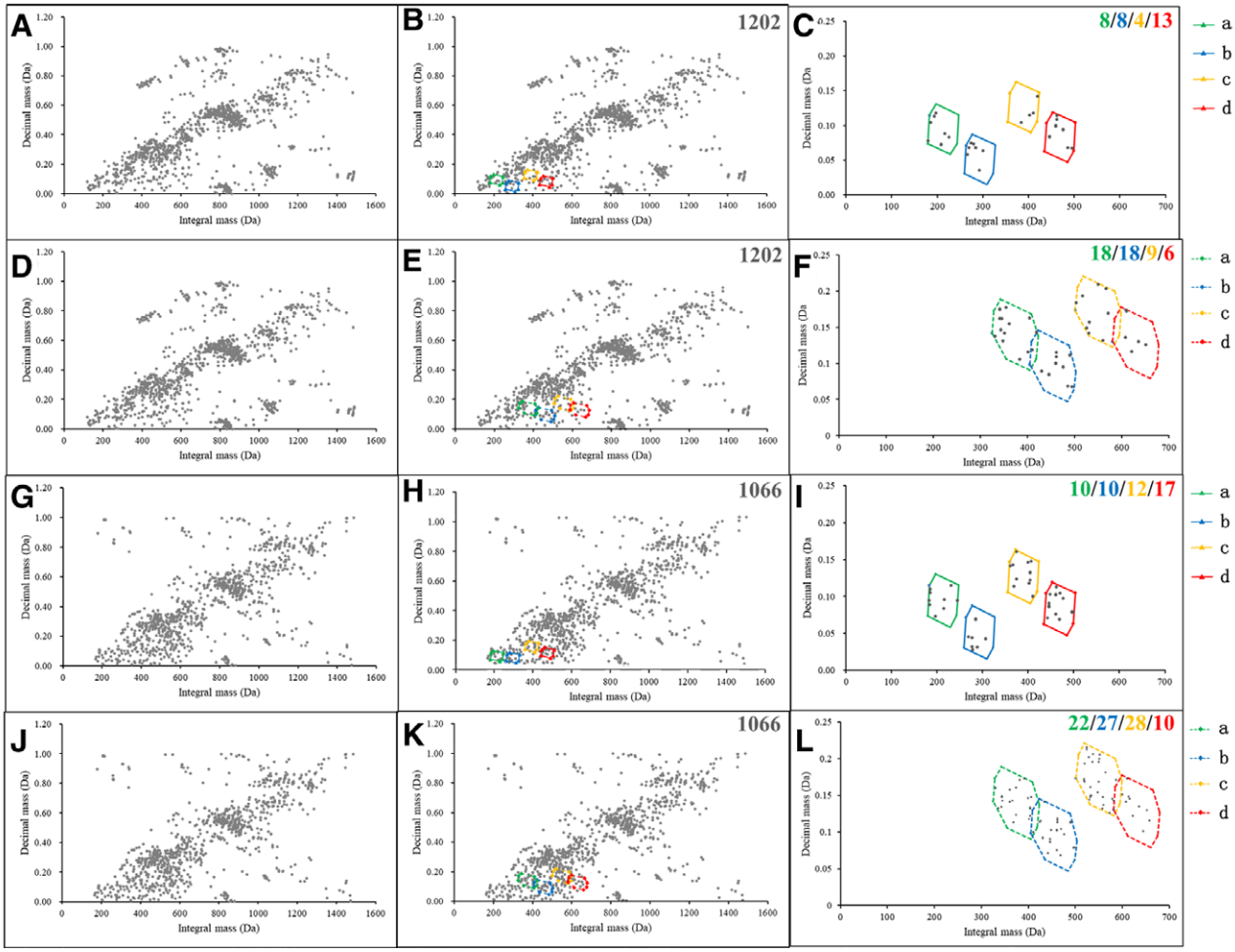

Figure 4. The process of screening potential iridoids by MDF. (A–C) The process of screening potential iridoid aglycones in positive mode. (D–F) The process of screening potential iridoid glycosides in positive mode. (G–I) The process of screening potential iridoid aglycones in negative mode. (J–L) The process of screening potential iridoid glycosides in negative mode. MDF: Mass defect filtering.

Step2: MDF

Then, the masses of 1,202 and 1,066 compounds obtained in the previous step were divided into two parts (integral mass and decimal mass) to be filtered by using the heptagonal modified MDF window. Those masses located within the heptagonal target windows were regarded as the potential compounds *in vivo* metabolism of LOL.

For isoquinoline alkaloids (as shown in Figure 2), after filtering through four screening windows, there were 20, 18, 14, and 9 candidate compounds were obtained respectively by MDF windows. In short, 59 non-repetitive candidate ions were screened for isoquinoline alkaloids in a positive ion mode.

For flavonoid glycosides and aglycones, as shown in Figure 3. After filtering through four screening windows, in positive mode, 26, 16, 25, and 7 flavonoid aglycones candidate compounds were obtained, respectively, totaling 62 (after removing duplicate values); 37, 15, 8, and 2 flavonoid glycosides candidate compounds were obtained, respectively, totaling 57 (after removing duplicate values). In short, 52 non-repetitive candidate compounds were screened for flavonoids in a positive mode. In negative mode, 28, 27, 49, and 16 flavonoid aglycones candidate compounds were obtained, respectively, totaling 107 (after removing duplicate values); 64, 41, 16, and 3 flavonoid glycosides candidate compounds were obtained, respectively, totaling 100 (after removing duplicate values). In short, 142 non-repetitive candidate compounds were screened for flavonoids in negative mode.

For iridoid glycosides and aglycones, as shown in Figure 4. After filtering through four screening windows, in positive ion mode, 8, 8, 4, and 13 iridoid aglycones candidate compounds were obtained, respectively, totaling 33; 18, 18, 9, and 6 iridoid glycosides candidate compounds were obtained, respectively, totaling 50. In short, 67 non-repetitive candidate compounds were screened for iridoids in positive mode. In negative ion mode, 10, 10, 12, and 17 iridoid aglycones candidate compounds were obtained, respectively, totaling 49; and 22, 27, 28, and 10 iridoid glycosides candidate compounds were obtained, respectively, totaling 87 (after removing duplicate values). In short, 107 non-repetitive candidate compounds were screened for iridoids in negative mode.

Step3: matching with database

In addition to flavonoids, isoquinoline alkaloids, and iridoids, other potential compounds were also identified using a matching method with a self-built database containing prototypes and their related metabolites.

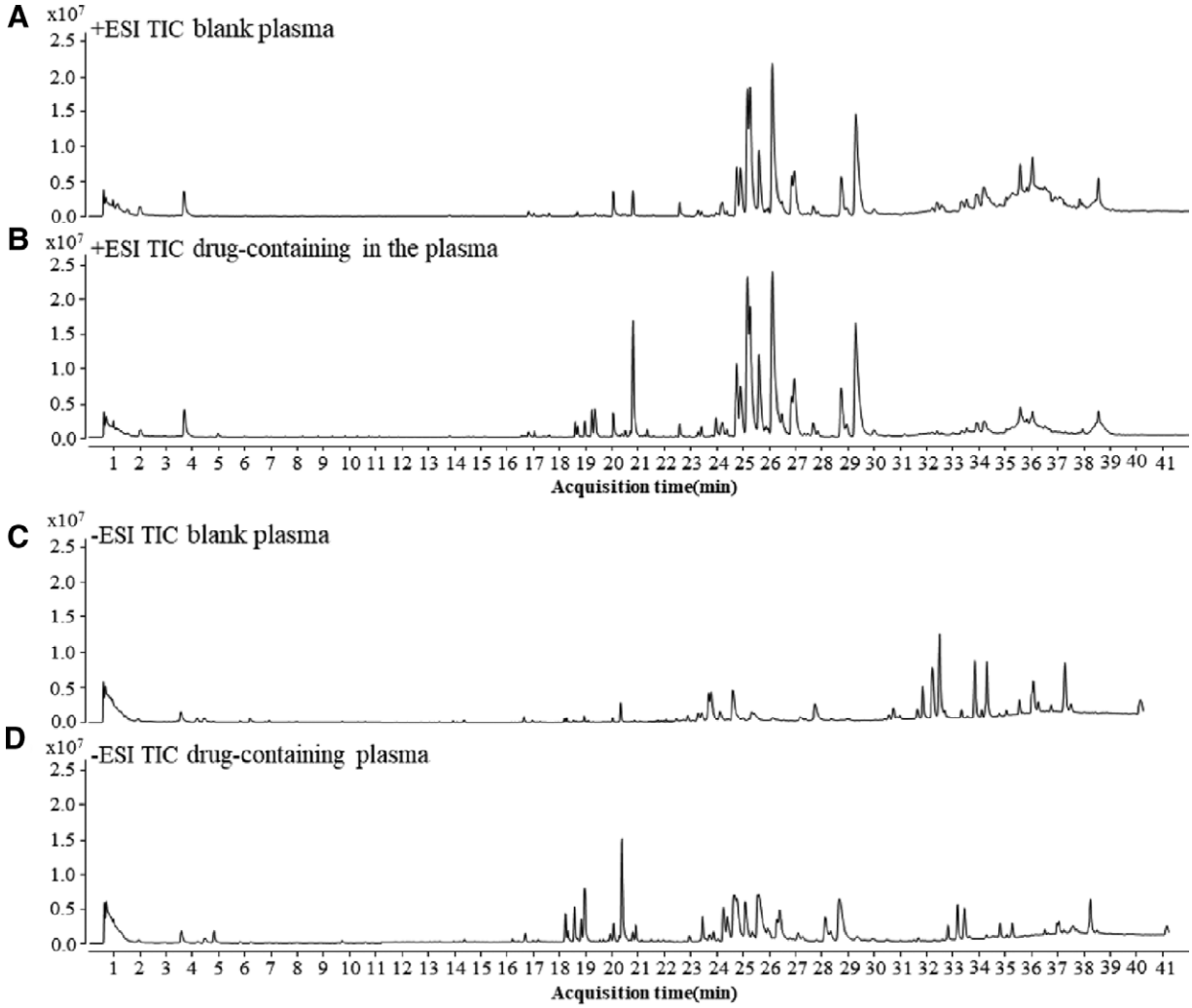

Figure 5. TICs obtained from the blank plasma (A, C) and drug-containing plasma (B, D) in the positive and negative ion modes, respectively. ESI: Electrospray ionization source; TICs: Total ion chromatograms.

Matched mass accuracy was set to ±10 ppm. The self-built database contains 710 compounds from five original medicinal materials and a total of 44,730 potential prototypes or metabolites produced by 62 phase I and phase II metabolic reactions of these 710 compounds[28]. The matching results showed that 236 and 281 potential compounds were retained in the positive and negative modes, respectively. These retained compounds were considered potential suspect compounds and would be further confirmed by MS/MS spectrum and multiple network databases.

Characterization of prototypes and metabolites in rat plasma

The mass spectrometry characteristics of the identified characteristic compounds in LOL provide a chemical basis for inferring their *in vivo* metabolic pathways and identifying metabolites. The identification of prototypes and metabolites in biological samples is often challenging due to interference from endogenous substances, low concentrations, and difficulty in predicting metabolic pathways. The method of utilizing mass profiler professional for background deduction and MDF can effectively reduce matrix interference and significantly increase the possibility of screening for minor metabolites. The proposed strategy constructs a compound library from the compounds identified from LOL and their potential metabolites to establish a foundation for the preliminary characterization of prototypes and metabolites in biological samples. In rat plasma, 159 compounds, including 58 prototype compounds and 101 metabolites, were characterized, with 31 compounds identified as control substances. The total ion chromatograms (TICs) of LOL *in vivo* in positive and negative ion modes are shown in Figure 5 and the extracted ion chromatograms (EICs) of metabolites of LQL are shown in Supplementary Figure S2 (http://links.lww.com/AHM/A164). The detailed MS/MS information of all components is shown in Supplementary Table S7 (http://links.lww.com/AHM/A164), and the chemical structures of 58 identified prototypes are exhibited in Supplementary Figure S1 (http://links.lww.com/AHM/A164).

Identification of flavones-related metabolites in plasma

In this research, 74 ingredients were characterized as flavonoids, consisting of 23 prototype compounds and 51 metabolites. The characterization results indicate that after oral administration of LOL, the main metabolic pathways of flavonoids in rats are sulfation and glucuronidation.

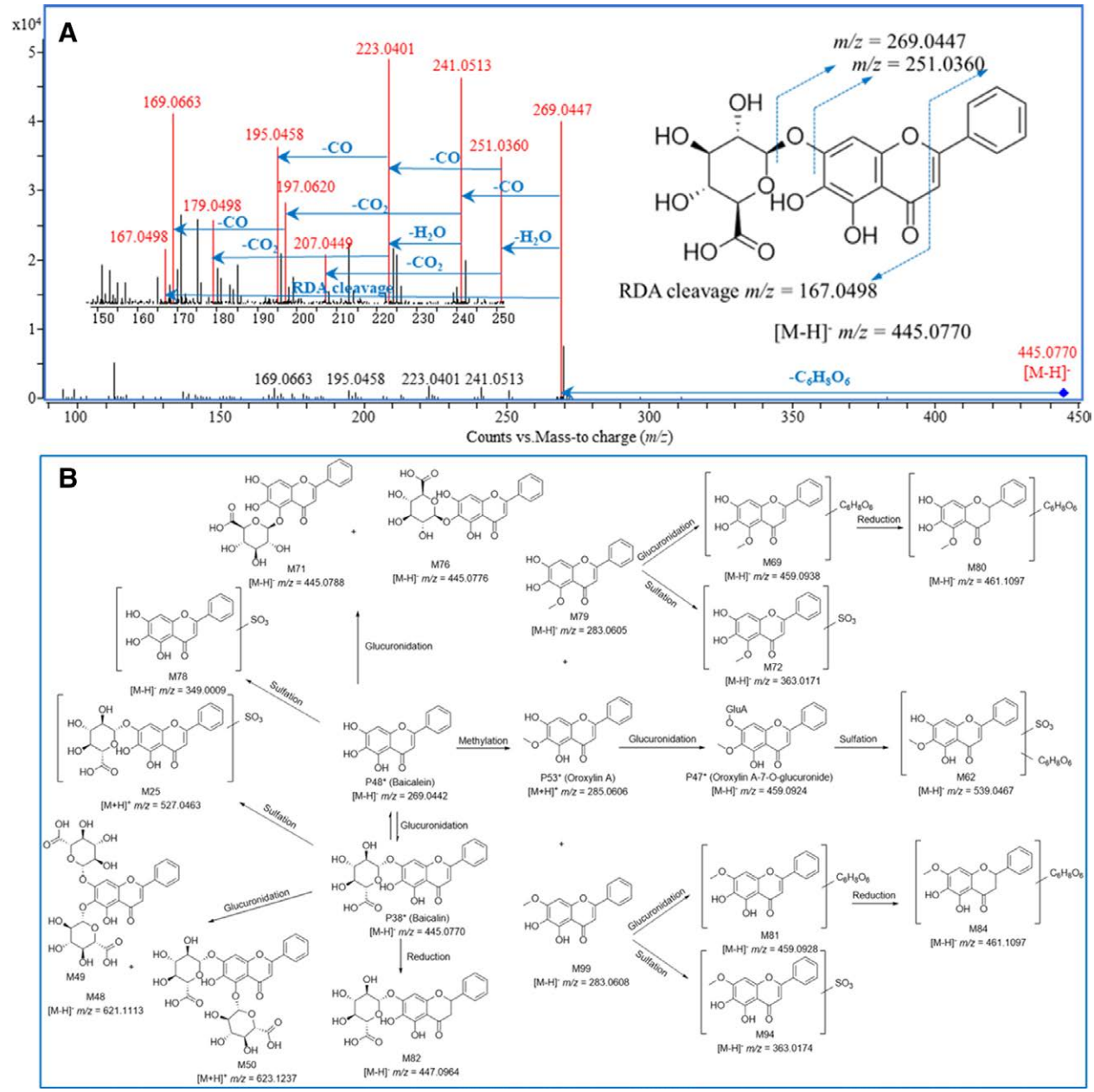

Figure 6. MS2 spectrum of baicalin (A) and its proposed metabolic pathways in rat plasma (B). RDA: Retro Diels-Alder reaction.

Taking baicalin (P38*) and its metabolites as an example, briefly explain the characterization process of flavonoids. For example, P48* (t_R = 14.84 minutes) showed a precursor ion $[M-H]^-$ at *m/z* 269.0442, which produced the same fragment ions 169.0666 and 269.0442 as P38*, indicating that the structures of P38* and P48*are similar. In addition, P48* exhibited the loss of $C_6H_8O_6$ which was 176 Da smaller than Baicalin (P38*). Therefore, it was identified as baicalin. Compounds M48 ($C_{27}H_{26}O_{17}$, *m/z* 621.1113, $[M-H]^-$, t_R = 10.38 minutes) had the similar fragment ions to P38* at *m/z* 445.0790 and *m/z* 269.0462. These fragments indicated that M48 was the glucuronidation product of P38*. Finally, it was presumably identified as baicalein-6, 7-di-O-glucuronide. Compound M25 ($C_{21}H_{18}O_{14}S$, *m/z* 527.0463, $[M + H]^+$) has the fragment ions at *m/z* 351.0140 $[M-C_6H_8O_6]^+$ and *m/z* 271.0590 $[M-C_6H_8O_6-SO_3]^+$, which was identified as the sulfate conjugation of P38*.

Besides, hydroxylation and methylation are also the main metabolic pathways of flavonoids. For instance, M79 and M99 exhibit the molecular ion $[M + H]^+$ at *m/z* 301.0698, matching the molecular formula $[C_{16}H_{11}O_4]^-$, and show the same product ion at *m/z* 268.0366. They were both 15 Da higher than that of baicalein, suggesting that M79 and M99 were the methylated metabolites of P48*. They were presumably identified as 5-O-methylbaicalein and 7-O-methylbaicalein, respectively.

From the perspective of metabolic pathways and metabolic profiles, after oral administration of LOL, the metabolites of flavonoids were rapidly produced and underwent glucuronidation and/or sulfation in rat plasma. In addition, metabolic pathways such as hydrogenation and methylation were also observed. The relevant metabolic reactions *in vivo* are shown in Figure 6.

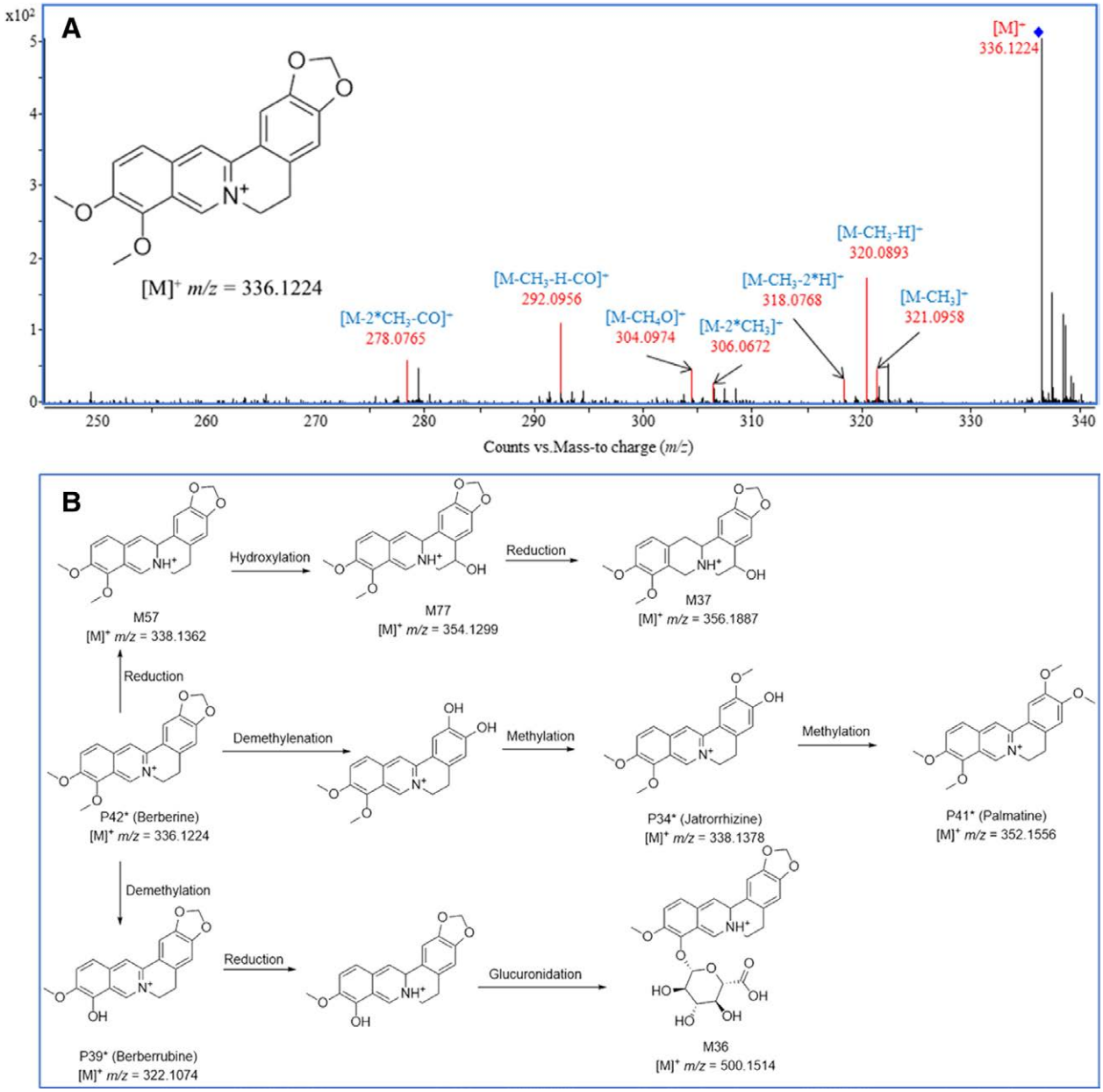

Figure 7. MS2 spectrum of berberine (A) and its proposed metabolic pathways in rat plasma (B).

Identification of isoquinoline alkaloids-related metabolites in rat plasma

A total of 30 alkaloids were tentatively characterized in plasma, consisting of 13 prototype compounds and 17 metabolites. After intragastric administration of the LOL in rats, the alkaloid prototype products detected in biological samples are mainly berberine, phellodendrine, magnoflorine, jatrorrhizine, etc. The results indicated that the primary types of alkaloid metabolism were hydroxylation, demethylation, demethylation, and/or glucuronidated conjugation. Herein berberine (P42*) and berberine-originated metabolites were chosen to explain the inference process of isoquinoline alkaloids.

Compound P42* ($C_{20}H_{18}NO_4^+$, *m/z* 336.1224, $[M]^+$) showed fragment ions at *m/z* 320.0893 $[M\text{-}CH_4]^+$, *m/z* 292.0956 $[M\text{-}CH_4\text{-}CO]^+$, and *m/z* 278.0765 $[M\text{-}CH_4\text{-}CO\text{-}CH_2]^+$, and was identified as berberine by reference. Compound M57 ($C_{20}H_{20}NO_4^+$, *m/z* 338.1362, $[M]^+$) had fragment ions at *m/z* 322.1126 $[M\text{-}CH_4]^+$, *m/z* 323.1051 $[M\text{-}CH_3]^+$, *m/z* 294.1073 $[M\text{-}CH_4\text{-}CO]^+$, and *m/z* 280.0880 $[M\text{-}CH_4\text{-}CO\text{-}CH_2]^+$, which was determined as reduction product of P42*. Compound M77 ($C_{20}H_{20}NO_5^+$, *m/z* 354.1299, $[M]^+$) showed fragment ion at *m/z* 336.1218 $[M\text{-}H_2O]^+$, *m/z* 322.1102 $[M\text{-}H_2O\text{-}CH_2]^+$, *m/z* 308.0901 $[M\text{-}H_2O\text{-}CH_2]^+$, which was determined as hydroxylation product of M57. Compound M36 ($C_{25}H_{26}NO_{10}^+$, *m/z* 500.1514, $[M]^+$) showed fragment ions at *m/z* 324.1204 $[M\text{-}C_6H_8O_6]^+$, *m/z* 309.0943 $[M\text{-}C_6H_8O_6\text{-}CH_3]^+$. And the ion at *m/z* 324.1204 was 12 Da lower than that of P42* (*m/z* 336.1224). Those reminded us that M36 probably existed in a multiple metabolic form of demethylation, reduction, and glucuronidation of P42*.

Overall, for the metabolites of isoquinoline alkaloids, this study mainly observed glucuronidation, hydroxylation, methylation, and reduction products in the plasma of rats after oral administration of LOL (as shown in Figure 7).

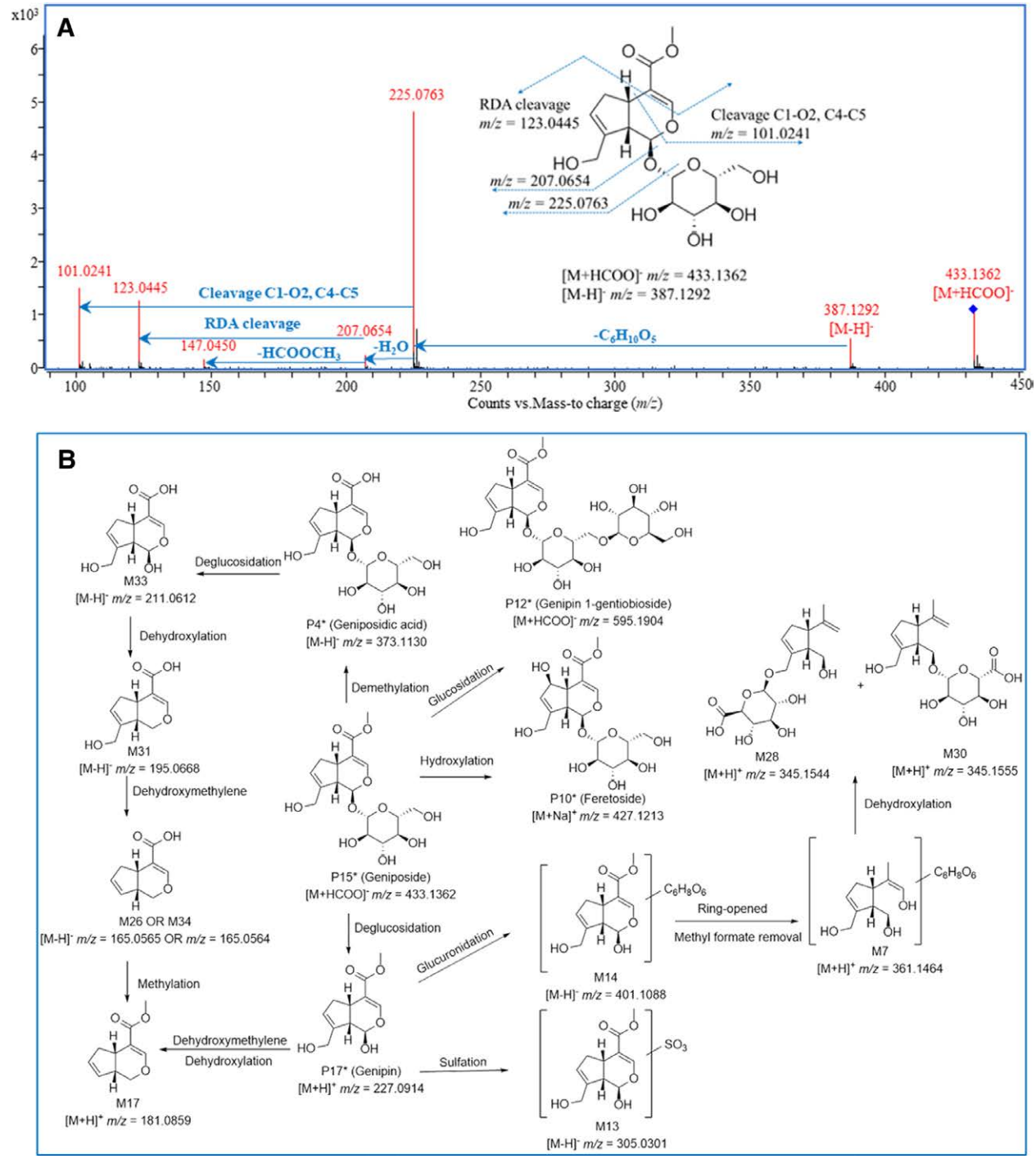

Figure 8. MS2 spectrum of geniposide (A) and its proposed metabolic pathways in rat plasma (B).

Identification of iridoids-related metabolites in rat plasma

A sum of 34 iridoids was tentatively characterized in plasma, consisting of 12 prototype compounds and 22 metabolites. After intragastric administration of the LOL in rats, the iridoid prototype products detected in biological samples are mainly geniposide, genipin, genipin-1-gentiobioside, geniposidic acid, etc. The research results indicate that iridoids are typically metabolized into dehydroxylation, demethylation, glucuronidation, and sulfonation products.

For instance, compound P15* generated a molecular formula of $C_{17}H_{24}O_{10}$ by an $[M + HCOO]^-$ ion at *m/z* 433.1362, and the MS/MS characteristic ions were *m/z* 225.0763 ($[M\text{-}C_6H_{10}O_5]^-$), *m/z* 207.0654 ($[M\text{-}C_6H_{10}O_5\text{-}H_2O]^-$), *m/z* 147.0450 ($[M\text{-}C_6H_{10}O_5\text{-}H_2O\text{-}CH_4O_2]^-$). By comparing with the MS/MS spectra of standard references, P15* was identified as Geniposide. In contrast, compound M13 ($C_{11}H_{14}O_8S$, *m/z* 305.0331, $[M\text{-}H]^-$) generated product ions at *m/z* 225.0767 $[M\text{-}SO_3]^-$, *m/z* 207.0661 and *m/z* 147.0445, which was identified as a sulfur conjugate of genipin (P17*). Compound M14 ($C_{17}H_{22}O_{11}$, *m/z* 401.1088, $[M\text{-}H]^-$) showed fragment ions at *m/z* 225.0753 $[M\text{-}C_6H_8O_6]^-$, *m/z* 207.0621, and *m/z* 147.0436, which was recognized as the monoglucuronide coupling of genipin. Furthermore, glucuronidation can also occur on the hydroxyls at the C-1

and C-10 positions. Compound M7 ($C_{16}H_{24}O_9$, *m/z* 361.1464, $[M + H]^+$) afforded the product ions at *m/z* 185.1160 $[M\text{-}C_6H_8O_6]^+$, *m/z* 167.1030 $[M\text{-}C_6H_8O_6\text{-}H_2O]^+$, and *m/z* 137.0935 $[M\text{-}C_6H_8O_6\text{-}H_2O\text{-}CH_2O]^+$, which was determined to be a ring-opening and methyl formate-removing derivative of M14.

For the metabolic types of iridoids, glucuronidation, sulfation, demethylation, and hydroxylation were mainly observed in rat plasma after oral administration of LOL (as shown in Figure 8).

Conclusions

The composition of LOL is complex, containing a large number of various natural small molecule compounds with rich pharmacological activities. For the first time, the *in vivo* metabolic profiles of natural small-molecular compounds in LOL were systematically examined in this study. An analysis tactic was constructed with the guidance of biotransformation, to screen and identify metabolites in complex biological systems. One hundred and fifty-nine compounds were tentatively identified, including 58 prototypes and 101 metabolites, and 31 of them were identified with the reference standards. This integrated strategy can reveal the potential active ingredients in TCMs relatively reliably, efficiently, and comprehensively. The results of the study provide research directions for quality evaluation and control of LOL. In future studies, the pharmacokinetic behavior as well as the tissue distribution of these components can be further investigated to clarify the index components for LOL quality control.

Conflict of interest statement

The authors declare no conflict of interest.

Funding

None.

Author contributions

Yue-Yue Tan performed the experiments and drafted the manuscript. Meng-Yuan Wang contributed to data processing, manuscript writing, and revision. Yu-Nuo Fan participated in data analysis. Ya-Liu Fan and Ye Zhang were involved in research design. Bin Li contributed to manuscript revision. Yong-Xiang Wang participated in article supervision. Hua Yang and Ping Li conceived and designed the study, and provided overall supervision.

Ethical approval of studies and informed consent

The animal experiments were approved by the Department of Science and Technology Jiangsu Province (License No.: 2022-09-007).

Acknowledgments

None.

REFERENCES

[1] Qian J, Kai G. Application of micro/nanomaterials in adsorption and sensing of active ingredients in traditional Chinese medicine. *J Pharm Biomed Anal* 2020;190:113548.
[2] Chen XF, Wu YL, Chen C, et al. Identifying potential anti-COVID-19 pharmacological components of traditional Chinese medicine Lianhuaqingwen capsule based on human exposure and ACE2 biochromatography screening. *Acta Pharm Sin B* 2021;11:222–236.
[3] Ge Nan, Yan Guangli, Sun Hui, et al. Version updating of strategy for drug discovery based on effective constituents of traditional Chinese. Acupunct Herb Med.2023;3(3):158–179.
[4] Zheng M, Tian L, Huang HL, et al. Cost-effectiveness analysis of traditional Chinese medicine for the treatment of upper respiratory tract infections: Yuxingcao Qinlan mixture versus LanQin oral liquid—a prospective study. *Eur J Integr Med* 2017;9:97–102.
[5] Wang HM, Hu WD, Wang HD, et al. Comprehensive multicomponent characterization and fingerprinting analysis of Lanqin Oral Liquid by ultra-high-performance liquid chromatography coupled with ion mobility-quadrupole time-of-flight mass spectrometry. *J Sep Sci* 2021;44(22):4111–4122.
[6] Fan YL, Liu RZ, Tan Q, et al. A database-guided integrated strategy for comprehensive chemical profiling of traditional Chinese medicine. *J Chromatogr A* 2022;1674:463145.
[7] Tian TT, Jin YR, Ma YH, et al. Identification of metabolites of oridonin in rats with a single run on UPLC-Triple-TOF-MS/MS system based on multiple mass defect filter data acquisition and multiple data processing techniques. *J Chromatogr B* 2015;1006: 80–92.
[8] Zeng SL, Duan L, Chen BZ, et al. Chemicalome and metabolome profiling of polymethoxylated flavonoids in Citri Reticulatae Pericarpium based on an integrated strategy combining background subtraction and modified mass defect filter in a Microsoft Excel Platform. *J Chromatogr A* 2017;1508:106–120.
[9] Zhang H, Zhang D, Ray K, et al. Mass defect filter technique and its applications to drug metabolite identification by high-resolution mass spectrometry. *J Mass Spectrom* 2009;44:999–1016.
[10] Zhang J, Huang ZH, Qiu XH, et al. Neutral fragment filtering for rapid identification of new diester-diterpenoid alkaloids in roots of Aconitum carmichaeli by ultra-high-pressure liquid chromatography coupled with linear ion trap-orbitrap mass spectrometry. *PLoS One* 2012;7:e52352.
[11] Li J, Wen Q, Feng Y, et al. Characterization of the multiple chemical components of Glechomae Herba using ultra high performance liquid chromatography coupled to quadrupole-time-of-flight tandem mass spectrometry with diagnostic ion filtering strategy. *J Sep Sci* 2019;42:1312–1322.
[12] Yang M, Zhou Z, Guo DA. A strategy for fast screening and identification of sulfur derivatives in medicinal Pueraria species based on the fine isotopic pattern filtering method using ultra-high-resolution mass spectrometry. *Anal Chim Acta* 2015;894:44–53.
[13] Yu Y, Yao C, Guo DA. Insight into chemical basis of traditional Chinese medicine based on the state-of-the-art techniques of liquid chromatography-mass spectrometry. *Acta Pharm Sin B* 2021;11:1469–1492.
[14] Blaženović I, Kind T, Ji J, et al. Software tools and approaches for compound identification of LC-MS/MS data in metabolomics. *Metabolites* 2018;8:31.
[15] Lai H, Ouyang Y, Tian G, et al. Rapid characterization and identification of the chemical constituents and the metabolites of Du-zhi pill using UHPLC coupled with quadrupole time-of-flight mass spectrometry. *J Chromatogr B Analyt Technol Biomed Life Sci* 2022;1209:123433.
[16] Zhang JY, Cai W, Zhou Y, et al. Profiling and identification of the metabolites of baicalin and study on their tissue distribution in rats by ultra-high-performance liquid chromatography with linear ion trap-Orbitrap mass spectrometer. *J Chromatogr B Analyt Technol Biomed Life Sci* 2015;985:91–102.
[17] Song JW, Long JY, Xie L, et al. Applications, phytochemistry, pharmacological effects, pharmacokinetics, toxicity of Scutellaria baicalensis Georgi. and its probably potential therapeutic effects on COVID-19: a review. *Chin Med* 2020;15:102.
[18] Du LY, Qian DW, Shang EX, et al. UPLC-Q-TOF/MS-based screening and identification of the main flavonoids and their metabolites in rat bile, urine and feces after oral administration of Scutellaria baicalensis extract. *J Ethnopharmacol* 2015;169: 156–162.

[19] Wang HY, Yan GL, Zhang AH, et al. Rapid discovery and global characterization of chemical constituents and rats metabolites of Phellodendri amurensis cortex by ultra-performance liquid chromatography-electrospray ionization/quadrupole-time-of-flight mass spectrometry coupled with pattern recognition approach. *Analyst* 2013;138(11):3303–3312.
[20] Zhang FX, Yuan YL, Cui SS, et al. Characterization of metabolic fate of phellodendrine and its potential pharmacological mechanism against diabetes mellitus by ultra-high-performance liquid chromatography-coupled time-of-flight mass spectrometry and network pharmacology. *Rapid Commun Mass Spectrom* 2021;35(18):e9157.
[21] Wang HY, Sun H, Zhang AH, et al. Rapid identification and comparative analysis of the chemical constituents and metabolites of Phellodendri amurensis cortex and Zhibai dihuang pill by ultra-performance liquid chromatography with quadrupole TOF-MS. *J Sep Sci* 2013;36(24):3874–3882.
[22] Han H, Yang L, Xu Y, et al. Identification of metabolites of geniposide in rat urine using ultra-performance liquid chromatography combined with electrospray ionization quadrupole time-of-flight tandem mass spectrometry. *Rapid Commun Mass Spectrom* 2011;25(21):3339–3350.
[23] Zhou J, Zhang YJ, Li N, et al. A systematic metabolic pathway identification of Common Gardenia Fruit (Gardeniae Fructus) in mouse bile, plasma, urine and feces by HPLC-Q-TOF-MS/MS. J. Chromatogr. *B Analyt Technol Biomed Life Sci* 2020;1145:122100.
[24] Wang K, Feng XC, Chai LW, et al. The metabolism of berberine and its contribution to the pharmacological effects. *Drug Metab Rev* 2017;49(2):139–157.
[25] Liu YT, Hao HP, Xie HG, et al. Oxidative demethylenation and subsequent glucuronidation are the major metabolic pathways of berberine in rats. *J Pharm Sci* 2009;98(11):4391–4401.
[26] Liu LM, Wang YT, Zhang JC, et al. Advances in the chemical constituents and chemical analysis of Ginkgo biloba leaf, extract, and phytopharmaceuticals. *J Pharm Biomed Anal* 2021;193:113704.
[27] Wang H, Sun YT, Guo W, et al. Identification and high-throughput quantification of baicalein and its metabolites in plasma and urine. *J Ethnopharmacol* 2023;301:115853.
[28] Gong P, Cui N, Wu L, et al. Chemicalome and metabolome matching approach to elucidating biological metabolic networks of complex mixtures. *Anal Chem* 2012;84(6):2995–3002.